Inorganic Chemistry

Article

pubs.acs.org/IC

Ruthenium(II) Complexes Bearing a Naphthalimide Fragment: A Modular Dye Platform for the Dye-Sensitized Solar Cell

Dmitry V. Pogozhev, Máté J. Bezdek, Phil A. Schauer, and Curtis P. Berlinguette*

Department of Chemistry and Centre for Advanced Solar Materials, University of Calgary, 2500 University Drive N.W., Calgary, Canada T2N 1N4

Supporting Information

ABSTRACT: Cycloruthenated complexes of the type $[Ru^{II}(N^{\wedge}N)_2(C^{\wedge}N)]^+$ ($N^{\wedge}N$ = substituted 2,2′-bipyridine; $C^{\wedge}N$ = substituted 3-(2′-pyridyl)-1,8-naphthalimide ligand) are shown to generate high power conversion efficiencies (PCEs) in the dye-sensitized solar cell (DSSC). It is shown that substitution of the pyridine ring of the $C^{\wedge}N$ ligand with conjugated groups can enhance molar absorption extinction coefficients, while the electron density imparted on the metal center is alleviated by the 1,8-naphthalimide fragment. This latter feature maintains a Ru(III)/Ru(II) redox couple more positive than 0.8 V versus NHE, thereby accommodating regeneration of the oxidized dye by an iodide-based redox mediator. This dye platform can consequently be modulated at various sites to enhance light absorption and suppress recombination between the redox mediator and the TiO_2 surface without compromising dye regeneration, thereby maintaining device PCEs as high as 7%. We also introduce a new phosphine-based coadsorbent, bis(2-ethylhexyl)phosphinic acid (BEPA), which is significantly easier to synthesize than the widely used bis(3,3-dimethylbutyl)phosphinic acid (DINHOP) while also facilitating high dye loading.

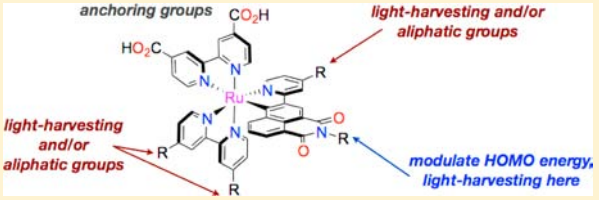

INTRODUCTION

There have been a number of significant recent advances in chromophore design for the dye-sensitized solar cell (DSSC),[1,2] including the discovery of high performance metal-free dyes[3,4] and a porphyrin-based dye[5] that produces a power conversion efficiency (PCE) in excess of 12% in the DSSC.[6] These findings followed the discovery that isothiocyanate-free ruthenium(II) dyes, such as $[Ru(dcbpy)_2(ppy)]^{1+}$ (**1a**; dcbpy = 4,4′-dicarboxy-2,2′-bipyridine; ppy =2-phenylpyridine), exhibit high PCEs in the DSSC.[7] This finding is particularly important from a commercial perspective because the lability of the NCS^- ligands that constitute conventional DSSC dyes, such as $[Ru(dcbpy)_2(NCS)_2]$ (**N3**), has been shown to be a source of degradation in the device.[8,9] Consequently, the ability to reach high PCEs with dyes bearing chelating ligands[10] (e.g., **1a**) in place of NCS^- groups offers enormous opportunities for enhancing the long-term stability of the DSSC.[11−14] Moreover, cycloruthenated dyes related to **1a** offer the opportunity to attenuate *both* the ground- and excited-state reduction potentials through judicious substitution of the aryl ring (Figure 1).[15] This same procedure does not translate effectively to **N3** because the highest occupied molecular orbital (HOMO) is delocalized over the isothiocyanato groups, which cannot be as easily functionalized.

A major focus of our program (and others[16−24]) has been centered on developing ruthenium complexes bearing anionic chelating ligands, such as deprotonated forms of ppy and 6-phenyl-2,2′-bipyridine.[14,25] One of the fundamental issues with these types of dyes in conventional DSSCs, however, is the need to maintain a metal-centered reduction potential positioned more positively than +0.8 V vs NHE (all electrochemical potentials in this manuscript are referenced versus NHE) so that regeneration by the redox mediator is a thermodynamically favorable process.[6,26,27] [The relevant one-electron redox couple here is likely $I^{\bullet}/I^-$ ($E^{\circ} \sim +0.8$ V); note that the I^-/I_3^- couple at 0.4 V that defines the voltage of the cell is a two-electron couple catalyzed by the counter-electrode.[28]] Consequently, electron-withdrawing groups (EWGs) on the aryl ring of these types of dyes are usually needed in order to achieve high PCEs.[7,11,20] Unfortunately, this prerequisite imposes significant constraints on how the balance of the dye scaffold may be designed (e.g., electron-rich light-harvesting substituents on a polypyridyl ligand can shift the HOMO energy too negative to be regenerated by I^-),[29] thereby prompting us to seek out more weakly σ-donating anionic ligands.

Following this line of inquiry, we report herein a new class of cycloruthenated compounds that consist of a naphthalimide fragment[31] (Figure 1 and Chart 1). We view this class of sensitizer to be a platform for sensitizing TiO_2 because the metal-based oxidation potentials are sufficiently positive in energy (i.e., >+0.8 V) to enable the structure (e.g., -R, $-R_1$, and $-R_2$ in Chart 1) to be manipulated without compromising DSSC performance. Moreover, the electron-rich portion of the molecule can be modulated to potentially affect chemical interactions with the electrolyte. The new opportunities for optimizing both the light-harvesting properties and dye

Received: November 9, 2012
Published: February 25, 2013

   dx.doi.org/10.1021/ic3024524 | Inorg. Chem. 2013, 52, 3001−3006

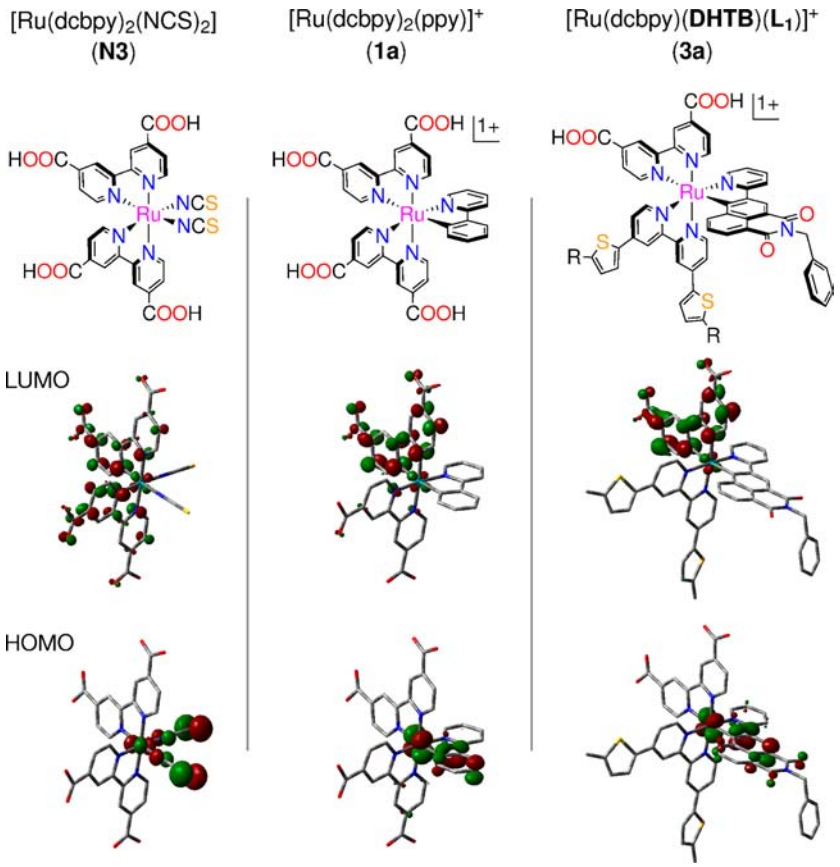

Figure 1. Three classes of ruthenium-based DSSC sensitizers illustrating the similarities of the frontier molecular orbitals (orbital isosurfaces plotted at 0.05 au; **DHTB** = 4,4′-(5″-*n*-hexyl-2″-thienyl)-2,2′-bipyridine, methyl analogue of **DHTB** shown for simplicity; $\mathbf{HL_1}$ = *N*-benzyl-3-(2′-pyridyl)-1,8-naphthalimide).[7,11,30]

regeneration steps offered by these novel organometallic sensitizers, which can reach PCEs that exceed that of champion dyes measured under the same conditions, are outlined below.

RESULTS AND DISCUSSION

The cyclometalating proligands, *C*^*N*, for each of the title complexes were prepared by a Stille coupling of the relevant *N*-substituted-3-bromo-1,8-naphthalimide and 2-(trimethylstannyl) pyridine fragments in accordance with a previously reported procedure.[31] In cases where alkylthiophene substituents were used, a Suzuki cross-coupling scheme involving *N*-(3′,5′-dimethylphenyl)-3-(4′′,4′′,5′′,5′′-tetramethyl-1′′,3′′-dioxaborolan-2′′-yl)-1,8-naphthalimide and 2-chloro-4-(5'-hexylthiophen-2'-yl)-pyridine was needed to access the relevant *C*^*N* proligand. The reaction of these proligands with $[(\eta^6\text{-}p\text{-cymene})RuCl_2]_2$ or $[(\eta^6\text{-benzene})RuCl_2]_2$ furnished the cyclometalated precursor $[Ru(C\text{^}N)(MeCN)_4]^+$ as the major product; $[Ru(C\text{^}N)(\eta^6\text{-}p\text{-cymene})(MeCN)_2]^+$ was not formed in significant quantities when the former metal reagent was employed. The esterified derivative, **2**, of dye **2a** was isolated by reacting $[Ru(C\text{^}N)(MeCN)_4]^+$ with 2 equiv of 4,4′-dicarboxyethyl-2,2′-bipyridine (DCEB) in ethanol. The family of heteroleptic ruthenium complexes, **3**−**6**, were obtained by the synchronous addition of DCEB and 4,4′-bis(5′′-hexylthiophen-2′′-yl)-2,2′-bipyridine (DHTB) to the cyclometalated precursor in ethanol (Figure S5). These esterified derivatives, **2**−**6**, were converted to the corresponding dyes, **2a**−**6a**, in high yields, after being left to reflux in a $DMF/H_2O/Et_3N$ (3:1:1) mixture.

The UV−vis absorption spectra of the ester derivatives are shown in Figure 2a. The spectrum of **2** is characterized by an intense band centered at 544 nm (denoted λ_{max1}; $\varepsilon = 1.4 \times 10^4$ M^{-1} cm^{-1}), which, on the basis of TDDFT calculations for **2a**, we attribute predominantly to transitions from the naphthalimide fragment and substituent to the bipyridine ligands (see Supporting Information). The band centered at ∼415 nm (λ_{max2}; $\varepsilon = 1.2 \times 10^4$ M^{-1} cm^{-1}) bears greater MLCT character, wherein transitions to the bipyridyl fragments arise from both ruthenium- and naphthalimide-centered orbitals. Intense $\pi-\pi^*$ transitions dominate the spectrum at $\lambda < 350$ nm. Heteroleptic complexes **3**−**6** exhibit similar absorption profiles (λ_{max1} = 413−419 nm and λ_{max2} = 555−561 nm), but differ in absorption intensities (Figure 2, Table 1). Indeed, the superior light harvesting properties of **3**−**6** relative to **2** reveal the benefit of the two alkylthiophene units about the auxiliary bpy ligand. DFT calculations suggest the HOMO to reside predominantly on the ruthenium (*ca.* 30%) and naphthalimide (*ca.* 50%) fragments for complexes **3a**, **5a**, and **6a**, whereas the HOMO is localized on the electron-rich dimethoxyphenyl substituent in complex **4a**. Though not altering the overall absorption profile in comparison to the other title complexes, the decreased molar absorptivity of complex **4** is plausibly attributable to the shift in electron density away from the naphthalimide core and ruthenium center orbitals that dominate the UV−vis transitions. The presence or absence of a methylene spacer between the terminal substituent and core does not appear to significantly affect molecular absorption properties (**3** *cf.* **5**, Figure 2a), as is to be expected by the

dx.doi.org/10.1021/ic3024524 | *Inorg. Chem.* 2013, 52, 3001−3006

Chart 1. Numbering Scheme for the Cycloruthenated Complexes under Investigation

-R_1= -Et **(1)**
-R_1= -H **(1a)**

-R_1= -Et **(2)**
-R_1= -H **(2a)**

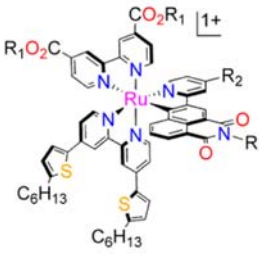

complex	substituent -R	-R_1	-R_2
3		-Et	-H
3a		-H	-H
4	OMe, OMe	-Et	-H
4a	OMe	-H	-H
5	OMe	-Et	-H
5a		-H	-H
6		-Et	C_6H_{13}
6a		-H	C_6H_{13}

absence of π-conjugation through the naphthalimide nitrogen atom. The inclusion of the 5-hexyl-2-thienyl moiety at the *para* position of the *C^N* pyridyl ring for complex **6** clearly results in enhanced light absorption, in agreement with (TD)DFT calculations for **6a** that show orbital character extended from the metal over the thienyl moiety (Figure 3). The MLCT band of **1** is bathochromically shifted relative to each of the title complexes, which corroborates the more weakly σ-donating character of the naphthalimide fragment relative to 2-phenylpyridine.

The corresponding acid derivatives, **2a**−**6a**, each exhibit similar spectroscopic characteristics although they do display different trends in intensities due largely to solubility issues. Complexes **2a**−**6a** are weakly emissive upon excitation at wavelengths corresponding to λ_{max1} and generate emission maxima over the λ = 737−757 nm range (Figure 2b, Table 1). The two compounds bearing a benzyl moiety appended to the naphthalimide fragment demonstrate two similar lifetimes (τ_1 = 17.59 and 9.36 ns and τ_2 = 65.96 and 67.73 ns for **2a** and **3a**, respectively), while **4a**−**6a** each demonstrates a single ∼65 ns lifetime.

The electrochemical behavior of **2**−**6** and the corresponding dyes were measured by cyclic voltammetry; square wave voltammograms of the dyes attached to TiO_2 were also evaluated (see Figure 4). A reversible one-electron oxidation process was observed at +1.17 V in the cyclic voltammogram (CV) for **2**. Of relevance to the DSSC is the fact that this value is shifted more positively by ∼200 mV relative to that of **1**. Consequently, the heteroleptic compounds **3**−**6**, which bear additional electron-rich light-harvesting units, exhibit reversible oxidation waves at *ca.* 1.05 V, a value that is still sufficiently positive to be regenerated by the relevant iodide-based redox mediator (i.e., >+0.8 V vs NHE). This potential is decreased by 50−100 mV upon saponification of the esters, but sufficiently positive values are still maintained. Successive one-electron reduction processes involving the DCEB and DHTB ligands were also observed for each complex (Table S1). The E_{0-0} (determined from intersections of the emission and absorption curves; Figure 2b) and $E(S^+/S)$ values for each of the dyes indicate $E(S^+/S^*)$ levels over the −0.88 to −1.00 V range for **2a**−**6a**, all of which are suitably positioned for efficient electron-injection into TiO_2.[32,33]

Current−voltage traces were collected on DSSCs constructed by immersing TiO_2 photoelectrodes in a solution containing dyes **1a**−**6a** (0.2 mM) in absolute ethanol (Table 2), and utilizing iodide-based electrolyte compositions [i.e., DMII (0.6M), NaI (0.6M), I_2 (0.06M), *t*-BP (0.5M), GuSCN (0.1M) in MeCN]. Chenodeoxycholic acid (CDCA) and the novel bis(2-ethylhexyl)phosphinic acid (BEPA; Figure 5) were each examined as coadsorbents in this study. The latter compound can be viewed as an analogue of the proven coadsorber, bis(3,3-dimethyl-butyl)phosphinic acid (DINHOP; Figure 5),[35,36] but BEPA has the distinct advantage of being easier to synthesize than DINHOP while facilitating higher dye loading than CDCA (*vide infra*).

Benchmark devices (using CDCA as the coadsorbent) reached PCE = 3.1% and PCE = 5.7% for **1a** and

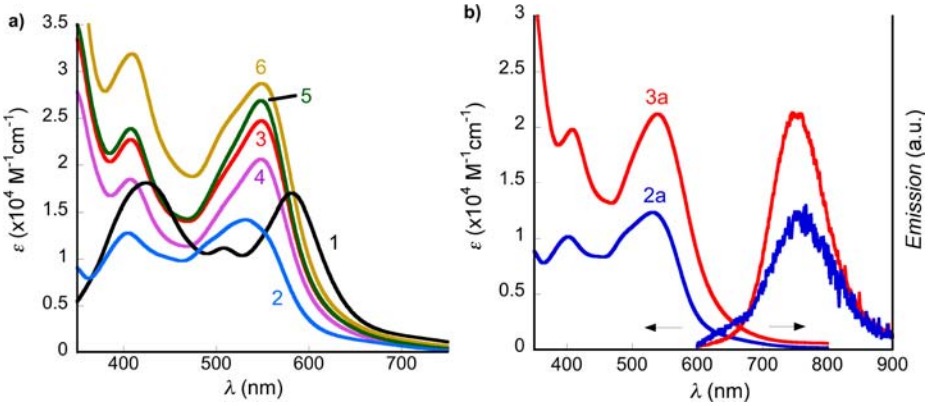

Figure 2. (a) UV−vis absorption spectra of **1**−**6** recorded in MeOH. (b) UV−vis absorption and ambient temperature emission spectra of **2a** and **3a** measured in MeOH.

dx.doi.org/10.1021/ic3024524 | *Inorg. Chem.* 2013, 52, 3001−3006

Table 1. Spectroscopic and Electrochemical Properties of Title Complexes[a]

	UV−vis data		emission data					
compd	λ_{max1} (nm)	λ_{max2} (nm)	τ^1 (ns)	τ^2 (ns)	χ^2	λ_{em} (nm)	E (S^+/S) (V vs NHE)	E (S^+/S^*) (V vs NHE)
1	582 (1.7)	505 (1.1)					+0.96	
1a	577 (1.2)	504 (1.0)				827[15]	+0.84	
2	544 (1.4)	415 (1.2)					+1.17	
2a	532 (1.2)	408 (1.0)	17.59	65.96	1.150	757	+1.09	−0.88
3	561 (2.5)	419 (2.2)					+1.05	
3a	540 (2.1)	408 (2.0)	9.36	67.73	1.006	751	+1.01	−0.89
4	555 (2.0)	413 (1.8)					+1.03	
4a	536 (1.8)	416 (1.6)	65.00		1.028	739	+0.90	−0.96
5	556 (2.6)	416 (2.3)					+1.03	
5a	547 (1.7)	420 (1.6)	66.53		1.031	743	+0.89	−1.00
6	557 (2.8)	415 (3.1)					+1.02	
6a	543 (2.4)	426 (2.5)	62.80		1.070	737	+0.89	−0.97

[a]UV−vis absorption data recorded in MeOH at 298 K. ε values indicated in parentheses with units of $\times 10^4$ M^{-1} cm^{-1}. Electrochemical data collected on glassy carbon electrode using 0.1 M $^nBu_4NBF_4$ DMF solutions at a scan rate of 200 mV/s and referenced to 1,1′,2,2′,3,3′,4,4′-octamethylferrocene $[oFc]^+/[oFc]$ internal standard followed by conversion to NHE ($[oFc]^+/[oFc]$ vs NHE = +0.29 V). Counterion is PF_6^- for all cationic complexes.

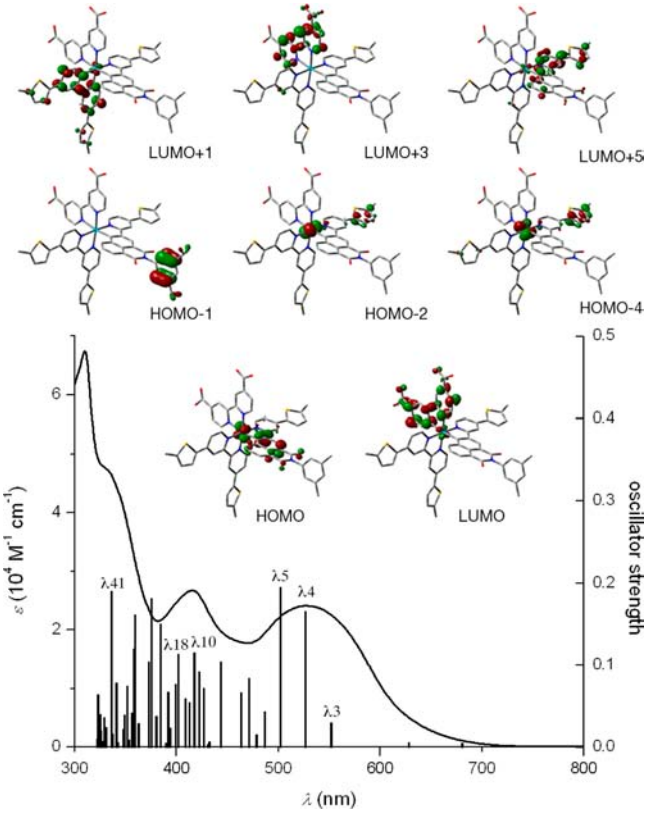

Figure 3. Calculated and experimental UV−vis absorption spectrum of **6a** with pertinent frontier molecular orbitals. Details of calculated transitions (theoretical wavelength in nm, oscillator strength, % contribution to transition): λ_3 HOMO → LUMO + 1 (552, 0.0303, 74%); λ_4 HOMO − 2 → LUMO (527, 0.1654, 77%); λ_5 HOMO − 1 → LUMO + 1 (502, 0.1951, 41%); λ_{10} HOMO − 1 → LUMO + 3 (443, 0.1040, 42%); λ_{18} HOMO − 1 → LUMO + 5 (402, 0.1139, 68%); λ_{41} HOMO − 4 → LUMO + 2 (336, 0.1900, 39%).

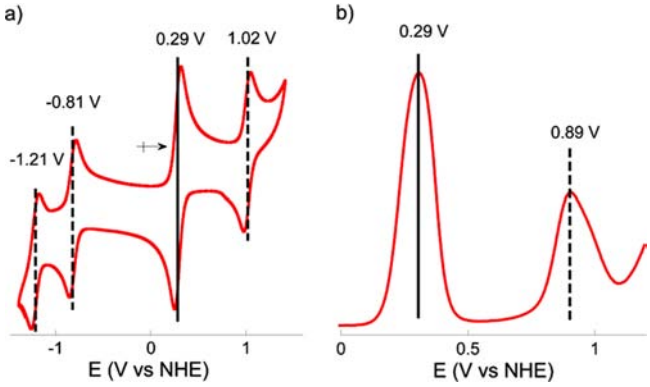

Figure 4. (a) Cyclic and (b) square wave voltammogram of **6** in solution and on TiO_2, respectively. Data was recorded in DMF in both cases, with the internal $[oFc]^+/[oFc]$ reference shown at +0.29 V vs NHE.

$[Ru(4,4′,4″\text{-tricarboxy-}2,2′:6′,2″\text{-terpyridine})(NCS)_3](Bu_4N)_3$ (black dye), respectively (Table 2). The title dyes **2a**−**6a** demonstrate comparably higher PCEs. The highest PCE (7.0% at 1 Sun; 7.3% at 0.6 Sun) was observed for the dye **6a**, characterized by the best optical properties and the lowest surface coverage. Notably, superior efficiencies were obtained with BEPA than with CDCA, a feature we ascribe to the higher surface coverage using the phosphine derivative.

While comparable PCEs were measured for **3a** and **5a** using CDCA, cell efficiencies were markedly lower for dye **4a**. Although the role of these −OMe groups remains under investigation, the finding casts light on the sensitivity of PCE to substituents about the anionic ligand. Dye **4a** notwithstanding, each of the heteroleptic dyes displayed higher PCEs relative to **2a**, a feature that is manifest in the additional light-harvesting units driving up the J_{sc} values. As expected, the alkyl substituents of the heteroleptic dyes enhance the V_{oc} values by impeding undesirable recombination processes. The incident-photon-to-current-efficiency (IPCE) traces for devices based on **3a** and **6a** are shown in Figure 6 and show an onset at *ca.* 780 nm with the highest response over the ∼450−600 nm range (maxima of 68.5% and 71.1% are observed at 540 and 530 nm, respectively). The congruent IPCE traces for these two complexes, taken together with the substantial V_{oc} increase in the case of **6a**, are consistent with the increase in PCE being a manifestation of the alkyl groups suppressing the recombination processes.

dx.doi.org/10.1021/ic3024524 | *Inorg. Chem.* 2013, 52, 3001−3006

Table 2. Photovoltaic Data Obtained for DSSCs Sensitized by 1a−6a Using Different Coadsorbents and at Different Light Intensities[a]

entry	dye	Sun	coadsorbent[1]	V_{oc} (V)	J_{sc} (mA cm^{-2})	FF	PCE (%)
1	**1a**	1	CDCA	0.53	8.49	0.53	3.1
2	**2a**	1	BEPA	0.59	13.6	0.59	4.8
3	**3a**	1	CDCA	0.65	16.3	0.56	6.3
4	**4a**	1	BEPA	0.60	9.9	0.64	3.9
5	**5a**	1	CDCA	0.70	14.5	0.65	6.6
6	**5a**	0.6	CDCA	0.68	10.1	0.67	7.0
7	**6a**	1	BEPA	0.68	15.4	0.65	7.0
8	**6a**	0.6	BEPA	0.66	10.3	0.68	7.3
9	black dye[34]	1	CDCA	0.68	13.77	0.59	5.7

[a]Electrolyte compositions used for device fabrication: DMII (1,3-dimethylimidazolium iodide) (0.6 M), NaI (0.6 M), I_2 (0.06 M), *t*-BP (4-tert-butylpyridine) (0.5 M), GuSCN (guanidinium thiocyanate) (0.1 M) in MeCN; 0.1 equiv of BEPA or 10 equiv of CDCA was used as coadsorbent as indicated. DSSC substrate consists of 12-μm active and 3-μm scattering TiO_2 layers; 0.28 cm^2 active area.

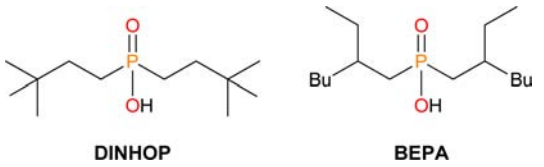

Figure 5. Chemical structures of bis(3,3-dimethyl-butyl)phosphinic acid (DINHOP) and bis(2-ethylhexyl)phosphinic acid (BEPA). It is shown that the latter acts as an effective coadsorbent in this study.

CONCLUSIONS

This study describes a series of cycloruthenated DSSC sensitizers ligated by substituted 3-pyridyl-1,8-naphthalimide. The physicochemical properties of this novel dye scaffold can be manipulated by modifying various sites of the complex while not sacrificing performance. The best performing dye of this particular series in the DSSC was found to be the tris-heteroleptic complex **6a**. This dye was decorated with light-harvesting alkylthienyl moieties on both the auxiliary bipyridine ligand and pyridyl-naphthalimide ligand to produce substantial extinction coefficients and to also suppress charge recombination processes. While the presence of three electron-rich substituents in most cycloruthenated sensitizers would push the HOMO level to unsatisfactorily high energies for regeneration of the photo-oxidized dye by iodide, the naphthalimide fragment is sufficiently electron-withdrawing to maintain a thermodynamically favorable regeneration process thus reaching a performance of 7.0% under AM1.5 sunlight. This fragment also presents the opportunity to examine whether the chemical reactivity of the R group (see Chart 1) can affect the regeneration step with the redox mediator, a point that will be elaborated in future studies. In addition to this new dye platform containing an uncommon cyclometalating ligand,[31] we also introduce here an effective new coadsorbent, BEPA, for use in the DSSC. This coadsorbent was found to be superior to the widely used CDCA in certain cases, and is more synthetically accessible than the DINHOP precursor that is also pervasive in the field. These collective findings are important advances for the sensitization of TiO_2 in energy conversion schemes.

ASSOCIATED CONTENT

Supporting Information

Synthetic and computational details, and full characterization of complexes and devices. This material is available free of charge via the Internet at http://pubs.acs.org.

AUTHOR INFORMATION

Corresponding Author

*E-mail: cberling@ucalgary.ca.

Notes

The authors declare no competing financial interest.

ACKNOWLEDGMENTS

This work was financially supported by the Canadian Natural Science and Engineering Research Council (NSERC), Canada Research Chairs, Canadian Foundation for Innovation (CFI), Alberta Ingenuity, Alfred P. Sloan Foundation, and the Canada School of Energy and Environment (CSEE).

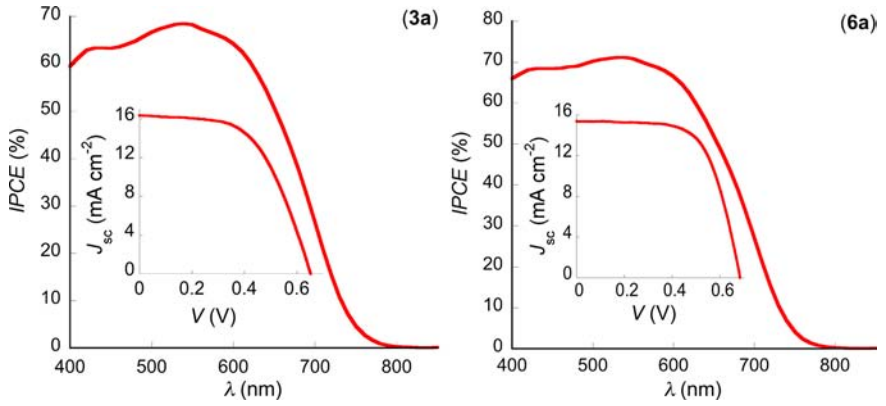

Figure 6. IPCE and photovoltaic (inset) data for **3a** (left) and **6a** (right).

dx.doi.org/10.1021/ic3024524 | *Inorg. Chem.* 2013, 52, 3001−3006

REFERENCES

(1) Hagfeldt, A.; Boschloo, G.; Sun, L.; Kloo, L.; Pettersson, H. *Chem. Rev.* **2010**, *110*, 6595.
(2) O'Regan, B.; Grätzel, M. *Nature* **1991**, *353*, 737.
(3) Hagberg, D. P.; Marinado, T.; Karlsson, K. M.; Nonomura, K.; Qin, P.; Boschloo, G.; Brinck, T.; Hagfeldt, A.; Sun, L. *J. Org. Chem.* **2007**, *72*, 9550.
(4) Zeng, W.; Cao, Y.; Bai, Y.; Wang, Y.; Shi, Y.; Zhang, M.; Wang, F.; Pan, C.; Wang, P. *Chem. Mater.* **2010**, *22*, 1915.
(5) Yella, A.; Lee, H.-W.; Tsao, H. N.; Yi, C.; Chandiran, A. K.; Nazeeruddin, M. K.; Diau, E. W.-G.; Yeh, C.-Y.; Zakeeruddin, S. M.; Grätzel, M. *Science* **2011**, *334*, 629.
(6) Robson, K. C. D.; Bomben, P. G.; Berlinguette, C. P. *Dalton Trans.* **2012**, *41*, 7814.
(7) Bessho, T.; Yoneda, E.; Yum, J.-H.; Guglielmi, M.; Tavernelli, I.; Imai, H.; Rothlisberger, U.; Nazeeruddin, M. K.; Grätzel, M. *J. Am. Chem. Soc.* **2009**, *131*, 5930.
(8) Likodimos, V.; Stergiopoulos, T.; Falaras, P.; Harikisun, R.; Desilvestro, J.; Tulloch, G. *J. Phys. Chem. C* **2009**, *113*, 9412.
(9) Asghar, M. I.; Miettunen, K.; Halme, J.; Vahermaa, P.; Toivola, M.; Aitola, K.; Lund, P. *Energy Environ. Sci* **2010**, *3*, 418.
(10) Djukic, J. P.; Sortais, J. B.; Barloy, L.; Pfeffer, M. *Eur. J. Inorg. Chem.* **2009**, 817.
(11) Bomben, P. G.; Gordon, T. J.; Schott, E.; Berlinguette, C. P. *Angew. Chem., Int. Ed.* **2011**, *50*, 10682.
(12) Chou, C.-C.; Wu, K.-L.; Chi, Y.; Hu, W.-P.; Yu, S. J.; Lee, G.-H.; Lin, C.-L.; Chou, P.-T. *Angew. Chem., Int. Ed.* **2011**, *50*, 2054.
(13) Hsu, C.-W.; Ho, S.-T.; Wu, K.-L.; Chi, Y.; Liu, S.-H.; Chou, P.-T. *Energy Environ. Sci.* **2012**, *5*, 7549.
(14) Bomben, P. G.; Robson, K. C. D.; Berlinguette, C. P. *Coord. Chem. Rev.* **2012**, *256*, 1438.
(15) Bomben, P. G.; Koivisto, B. D.; Berlinguette, C. P. *Inorg. Chem.* **2010**, *49*, 4960.
(16) Wadman, S. H.; Kroon, J. M.; Bakker, K.; Havenith, R. W. A.; van Klink, G. P. M.; van Koten, G. *Organometallics* **2010**, *29*, 1569.
(17) Wadman, S. H.; Kroon, J. M.; Bakker, K.; Lutz, M.; Spek, A. L.; van Klink, G. P. M.; van Koten, G. *Chem. Commun.* **2007**, 1907.
(18) Dragonetti, C.; Valore, A.; Colombo, A.; Roberto, D.; Trifiletti, V.; Manfredi, N.; Salamone, M. M.; Ruffo, R.; Abbotto, A. *J. Organomet. Chem.* **2012**, *714*, 88.
(19) Yao, C.-J.; Zhong, Y.-W.; Yao, J. *J. Am. Chem. Soc.* **2011**, *133*, 15697.
(20) Kim, J.-J.; Choi, H.; Paek, S.; Kim, C.; Lim, K.; Ju, M.-J.; Kang, H. S.; Kang, M.-S.; Ko, J. *Inorg. Chem.* **2011**, *50*, 11340.
(21) Singh, S. P.; Gupta, K. S. V.; Sharma, G. D.; Islam, A.; Han, L. *Dalton Trans* **2012**, *41*, 7604.
(22) Dixon, I. M.; Alary, F.; Heully, J.-L. *Dalton Trans* **2010**, *39*, 10959.
(23) Zhao, H. C.; Harney, J. P.; Huang, Y.-T.; Yum, J.-H.; Nazeeruddin, M. K.; Grätzel, M.; Tsai, M.-K.; Rochford, J. *Inorg. Chem.* **2011**, *51*, 1.
(24) Funaki, T.; Funakoshi, H.; Kitao, O.; Onozawa-Komatsuzaki, N.; Kasuga, K.; Sayama, K.; Sugihara, H. *Angew. Chem., Int. Ed.* **2012**, *51*, 7528.
(25) Bomben, P. G.; Robson, K. C. D.; Sedach, P. A.; Berlinguette, C. P. *Inorg. Chem.* **2009**, *48*, 9631.
(26) Boschloo, G.; Hagfeldt, A. *Acc. Chem. Res.* **2009**, *42*, 1819.
(27) Rowley, J. G.; Farnum, B. H.; Ardo, S.; Meyer, G. J. *J. Phys. Chem. Lett.* **2010**, *1*, 3132.
(28) Boschloo, G.; Gibson, E. A.; Hagfeldt, A. *J. Phys. Chem. Lett.* **2011**, *2*, 3016.
(29) Bomben, P. G.; Thériault, K. D.; Berlinguette, C. P. *Eur. J. Inorg. Chem.* **2011**, 1806.
(30) Nazeeruddin, M. K.; Kay, A.; Rodicio, I.; Humphry-Baker, R.; Mueller, E.; Liska, P.; Vlachopoulos, N.; Grätzel, M. *J. Am. Chem. Soc.* **1993**, *115*, 6382.
(31) Blanck, S.; Cruchter, T.; Vultur, A.; Riedel, R.; Harms, K.; Herlyn, M.; Meggers, E. *Organometallics* **2011**, *30*, 4598.
(32) Ardo, S.; Meyer, G. J. *Chem. Soc. Rev.* **2009**, *38*, 115.
(33) Listorti, A.; O'Regan, B.; Durrant, J. R. *Chem. Mater.* **2011**, *23*, 3381.
(34) Nazeeruddin, M. K.; Pechy, P.; Renouard, T.; Zakeeruddin, S. M.; Humphry-Baker, R.; Comte, P.; Liska, P.; Cevey, L.; Costa, E.; Shklover, V.; Spiccia, L.; Deacon, G. B.; Bignozzi, C. A.; Grätzel, M. *J. Am. Chem. Soc.* **2001**, *123*, 1613.
(35) Wang, M.; Li, X.; Lin, H.; Pechy, P.; Zakeeruddin, S. M.; Grätzel, M. *Dalton Trans* **2009**, 10015.
(36) Wang, M.; Plogmaker, S.; Humphry-Baker, R.; Pechy, P.; Rensmo, H.; Zakeeruddin, S. M.; Grätzel, M. *ChemSusChem* **2012**, *5*, 181.